Computers and Concrete, *Vol. 14, No. 3 (2014) 233-245*
DOI: http://dx.doi.org/10.12989/cac.2014.14.3.233

Fuzzy logic approach for estimating bond behavior of lightweight concrete

Mehmet E. Arslan*[1] and Ahmet Durmuş[2a]

[1]*Department of Civil Engineering*, *Düzce University*, *81620*, *Düzce*, *Turkey*
[2]*Department of Civil Engineering*, *Karadeniz Technical University*, *61080*, *Trabzon*, *Turkey*

(*Received January 20, 2014, Revised March 11, 2014, Accepted June 29, 2014*)

Abstract. In this paper, a rule based Mamdani type fuzzy logic model for prediction of slippage at maximum tensile strength and slippage at rupture of structural lightweight concretes were discussed. In the model steel rebar diameters and development lengths were used as inputs. The FL model and experimental results, the coefficient of determination R2, the Root Mean Square Error were used as evaluation criteria for comparison. It was concluded that FL was practical method for predicting slippage at maximum tensile strength and slippage at rupture of structural lightweight concretes.

Keywords: bond strength; bending; structural lightweight concrete; fuzzy logic approach

1. Introduction

Granulated slag is produced by quenching the liquid slag with a large amount of water to produce sand-like granulates. The granulates normally contain more than 95% of glass. Generally, they are ground to fine powder, called ground granulated blast furnace slag (GGBS). Using ground granulated blast furnace slag as a supplementary cementitious material in Portland cement concrete has many advantages, including improved durability, workability and economic benefits (Islam *et al*. 2014).

Compressive strength is the most important engineering property of concrete. Many experimental studies have been done about the development of compressive strength of slag blended concrete. Cheng *et al*. (2008) investigated strength development of slag blended concrete with different water to binder ratios and slag replacement ratios. Under standard curing conditions, at early age, slag blended concrete gain strength more slowly than Portland cement concrete. However, at late age, strength of slag blended concrete can surpass that of Portland cement concrete. Barnett *et al*. (2006) made experimental investigations on strength development of mortars containing ground granulated blast-furnace slag and Portland cement. Variables were the level of slag in the binder, water–binder ratio and curing temperature. They found that the early age strength is much more sensitive to temperature for higher levels of slag and the apparent activation energy increases approximately linearly with slag level. Oner and Akyuz (2007)

*Corresponding author, Assistant Professor, E-mail: E-mail: mehmeteminarslan@duzce.edu.tr
[a]Professor, E-mail: durmus@ktu.edu.tr

http://www.techno-press.org/?journal=cac&subpage=8 ISSN: 1598-8198 (Print), 1598-818X (Online)

presented a laboratory investigation on optimum level of ground granulated blast-furnace slag on the compressive strength of concrete. The test results proved that the compressive strength of concrete mixtures containing GGBS increases as the amount of GGBS increase. After an optimum point, at around 50% of the total binder content, the addition of GGBS does not improve the compressive strength. From references (Cheng *et al*. 2008; Barnett *et al*. 2006; Oner and Akyuz, 2007), it can be seen that the mechanical properties of slag blended concrete relate with both cement hydration and slag reaction. The development of compressive strength depends on many factors, such as age, water to binder ratio, slag replacement ratio, and curing conditions.

On the other hand, some models have been proposed to evaluate properties of hardening slag blended concrete. Douglas and Pouskouleli (1991) put forward a statistical design to describe the strength development of Portland cement-slag-fly ash mortars at various ages. With the experimental compressive strength values, a computerized statistical approach was used to find the equations governing strength development of the ternary systems at different ages. Brooks and Kaisi (1990) proposed a model to evaluate the early strength development of Portland and slag cement concretes cured at elevated temperatures. The development of strength under isothermal conditions was described by a hyperbolic expression equation, and the strength development for heat-cycled cured concrete was described using an equivalent isothermal temperature.

Contrasting to the empirical models of strength development of slag blended concrete (Douglas and Pouskouleli 1991; Brooks and Kaisi 1990), some hydration models have been built to predict mechanical-thermal-chemical-hydro properties of hardening slag blended concrete. Based on an extensive experimental research program on hardening slag blended concrete elements, De Schutter and Taerwe (1996) proposed a degree of hydration-based description for the compressive strength, Young's modulus, the uniaxial tensile strength, the splitting tensile strength, the flexural tensile strength, Poisson's ratio and the peak strain. Based on a multi-component hydration heat model and micro pore structure formation model, Song and Kwon (2009) evaluated chloride penetration in silica fume, fly ash and slag blended concrete using the diffusion coefficients obtained from a neural network algorithm. Similar with Song and Kwon (2009), based on computed micro pore structure, Yoon (2009) proposed a simple approach to calculate the diffusivity of concrete considering effects of tortuosity, micro-structural properties of hardened cement paste, and volumetric portion of aggregate. Most recently, Luan *et al*. (2012) proposed a hydration model of slag blended cement considering the role of calcium hydroxide as activator and the Ca/Si ratio of CSH. The influence of low Ca/Si ratio in the CSH inner product on slag reaction was taken into account using an enhanced slag reaction model. From references (De Schutter and Taerwe, 1996; Song and Kwon, 2009; Yoon, 2009; Luan *et al*., 2012), it can be seen that, based on the hydration model, the evolution of properties of hydrating cementitious materials can be described kinetically.

Due to the reaction between cement hydration and slag reaction, compared with ordinary Portland cement, the hydration of cement blended with slag is much more complex. As proposed by Luan *et al*. (2012), it is typical to consider the hydration reactions of cement and the blended mineral admixtures to model the hydration of blended concrete. In this paper, a numerical model is proposed to simulate the hydration of concrete containing slag. By considering the production of calcium hydroxide in cement hydration and its consumption during the reaction of mineral admixture, the reaction of slag is separated from that of cement hydration. The compressive strength development of hardening slag blended concrete is evaluated based on degree of hydration of cement and reaction degree of slag.

The contribution of this paper is relating the macro mechanical properties, i.e., development of compressive strength of blended concrete, with the evolution of microstructure of cement-slag blends. The parameters of cement hydration model, slag reaction model, and compressive strength development model are not changed when water to binder ratios and slag replacement ratios vary from one mix to the other. The physical meaning of these parameters is clear. Using the proposed calibration process in this paper, it is convenient for other researchers to use this hydration model. In addition, Oner and Akyuz (2007) reported that for concrete incorporating slag, after an optimum slag content, the addition of slag does not improve the compressive strength of concrete. In this paper, because the proposed model has taken into account the effect of slag replacement ratio on strength development, the proposed model can predict compressive strength development of concrete incorporating different slag contents. Furthermore, by comparing the strength development of slag blended concrete with that of Portland cement concrete, the optimum slag content can be analyzed.

2. Experimental details

In this study bond-slip behavior of SLWC in bending was experimentally investigated. For this purpose the experiments were carried out on totally 24 beam specimens, 12 for SLWC with 20ϕ development length and 12 for SLWC with 25ϕ development length. For each series bond behavior of steel rebars with 8, 10, 12, 14 mm diameters were tested.

2.1 Materials, mixture proportions and properties of concrete

SLWC was produced by using LWA of Eastern Black Sea Region. Physical properties of LWA are shown in Table 1. CEM-I/42.5 R was used as cement and dosage was kept constant at 350 kg/m3 with 0.5 w/c ratio. Mixture proportion of LWC is given in Table 2.

As stated before, 24-beam specimens were produced to investigate bond-slip behavior of SLWC. Before placing the concretes in the mold, steel rebars were covered with plastic cylinder to restrict the development length. Also 8 mm steel rebars were placed both sides of the rebars which will be tested. Purpose of using these rebars is to prevent bending and torsion of the rebars during the carrying of the beam specimens (Arslan 2007). Beam specimens used are shown in Fig. 1. In addition, three cylinder specimens were taken from all production of beams to determine and control mechanical properties of concretes. Physical and mechanical properties of SLWC are given in Table 3 and Table 4, respectively.

Table 1 Physical properties of LWA

Aggregate types	Aggregate size (mm)	Compressed unit weight (kN/m^3)	Loose unit weight (kN/m^3)	Specific gravity (kN/m^3)		Water absorption (%)
				Dry	Saturated	
LWA	Course > 4 mm	11.70	10.10	17.95	19.85	10.6
	Fine ≤ 4 mm	12.35	10.45	17.10	19.46	13.8

Table 2 Mix proportions of LWC

Material	Quantities of aggregates (kg/m^3) Sieve size (mm)					Saturation water (kg/m^3)	Mixing water (kg/m^3)	Cement (kg/m^3)
	0.5–1	1–2	2–4	4–8	8–16			
SLWC	208.1	208.1	208.1	346.9	416.3	169.28	175	350

Table 3 Physical properties of SLWC

Material	W/C	Specific gravity (kg/m3)			water absorption (%)
		Oven dry	Air dry	Saturated	
SLWC	0.5	1700	1810	1995	17

Table 4 Mechanical properties of SLWC

Material	W/C	fcm (MPa)	fck (MPa)	Ec (MPa)	Poisson Rat io	103* εco
SLWC	0.50	19.2	18.5	11.650	0.11	2.2


Fig. 1 Beam specimen

2.2 Test set-up

SBHBT enables to measure slips of the steel rebars by loading the beam at mid-point. Vertically applied loads and slips are measured by loadcell and LPDTs, respectively and they are recorded by data acquisition system. LPDTs with 0.013 mm precision are placed end points of the beam to measure slips of the steel rebar. Also a hinge is placed in the middle of the beam to ascertain the tensile forces more adequately (Arda 1968). Afterwards, yield, maximum and ultimate stresses are determined corresponding to the tensile forces at the steel rebars. Test set-up and implementing of the test are shown in Fig. 2 (Arslan 2007).

Bond stress which has 0.25 mm slippage was accepted as reliable bond stress (Ferguson 1965; Ersoy and Özcebe 2001; ACI 2005). Bond stress τ_b can be calculated as following;

$$\tau_{b=} f_s \cdot \phi / 4.1_b \tag{1}$$

Here, tensile stress, development length and rebar diameter are shown with f_s, lb and ϕ, respectively.

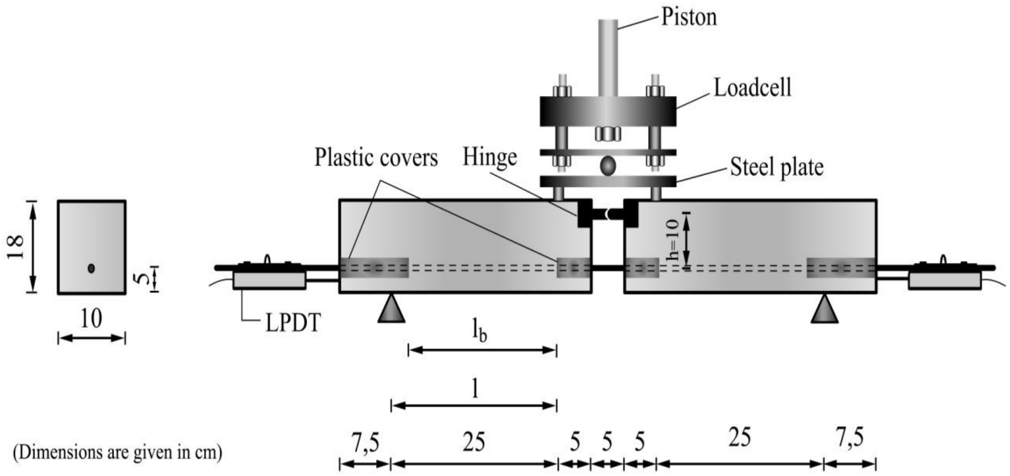

Fig. 2 Test set-up of standard Belgium hinged beam test and dimensions of specimens

3. Fuzzy logic theory and modelling steps

The main process of a general fuzzy inference system (FIS) includes four activities called as fuzzification, fuzzy rule base, fuzzy inference engine and defuzzification (Fig. 3). These parts are detailed below.

- Input: It contains all input parameters and information about them.
- Fuzzification: It converts each input data to degrees of membership by a lookup in one or more several membership function.
- Fuzzy rule base: This contains rules that include all possible fuzzy relation between input and outputs using IF-THEN format.
- Fuzzy Interference Engine: Collects all fuzzy rules in the fuzzy rule base and learns how to transform a set of inputs to related outputs.
- Defuzzification: This converts the resulting fuzzy outputs from fuzzy interference engine to a number (Akkurt *et al*. 2010).

There are two types of FIS that can be implemented in the MATLAB's FIS toolbox: Mamdani-type and Sugeno-type. Mamdani's method is the most commonly used fuzzy methodology and it expects the output Membership functions (MFs) to be fuzzy sets. After the aggregation process, there is a fuzzy set for each output variable that needs defuzzification (Köksal *et al*. 2012, Omid 2011).

Fuzzy expert system modeling can be pursued using the following steps (Abraham 2005).

- Select relevant input and output variables. Determine the number of linguistic terms associated with each input/output variable. Also, choose the appropriate family of membership functions, fuzzy operators, reasoning mechanism, and so on.
- Choose a specific type of fuzzy inference system (for example, Mamdani, Takagi–Sugeno etc.). In most cases, the inference of the fuzzy rules is carried out using the 'min' and 'max' operators for fuzzy intersection and union.

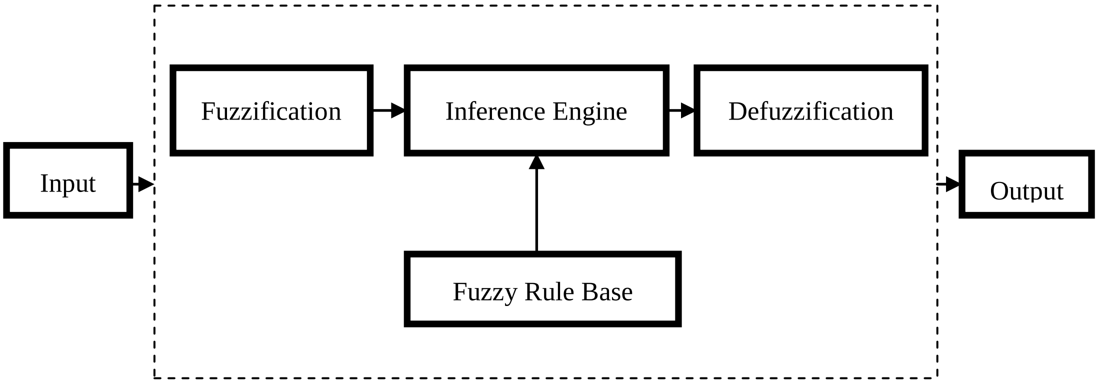

Fig. 3 Basic elements of FL

Design a collection of fuzzy if-then rules (knowledge base). To formulate the initial rule base, the input space is divided into multidimensional partitions and then actions are assigned to each of the partitions.

4. Application details of mamdani FL model, results and discussions

In this study, a rule based Mamdani type fuzzy logic model is used for prediction of slippage at maximum tensile strength (S_{su}) and slippage at rupture (S_{sr}) of structural lightweight concretes by using steel rebar diameters, maximum tensile stresses of steel rebars, tensile stresses of rupture and development lenghts of rebar as inputs. Flow diagram of the study is given in Fig. 4.

In the models, membership functions and their numerical ranges of the common input of two models are 4 triangular membership functions (trimf) and from 8 to 14 (mm) range of value for rebar diameters, 6 trimf and from 160 to 350 range of value for lb in both two models. The main difference of two models is that a different input and the outputs of the two models. The membership functions and their numerical ranges of the different inputs and outputs of two models are 5 trimf and from 416 to 580 range of value for F_{su} in MODEL I as input, 6 trimf and from 242 to 495 range of value for F_{sr} in MODEL II as input, 12 trimf and from 0 to 0.43 range of value for Ssu in MODEL I as output, 15 trimf and from 0 to 4.5 range of value for S_{sr} in MODEL II as output. General structure of the models is given in Fig. 5.

After determining membership functions details, 120 rules for Model I and 144 rules for Model II were formed using experimental results and experiences. Some of formed rules for two models are given Fig 7 a and b;

Output parameters variations as a function of inputs in the two models according to the formed rules are displayed in Fig. 8. These figures illustrate the relationship between inputs and outputs for two models.

There are five built-in methods supported: centroid, bisector, middle of maximum (the average of the maximum value of the output set), largest of maximum, and smallest of maximum. The most commonly used technique is the centroid defuzzification technique. This technique was used in order to determine crisp values of outputs for this study. The centroid defuzzification technique can be expressed as equation.

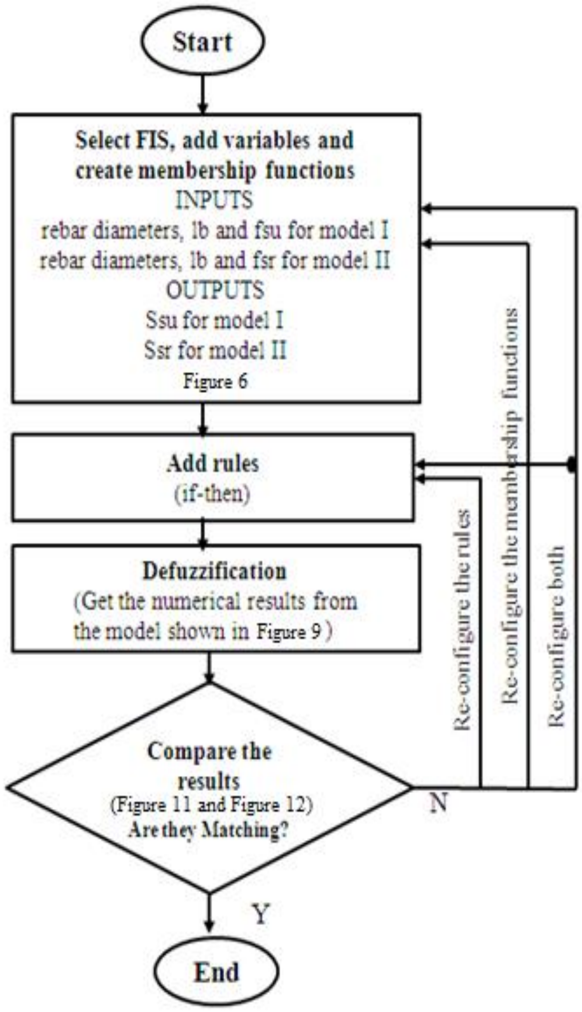

Fig. 4 Flow diagram for this study

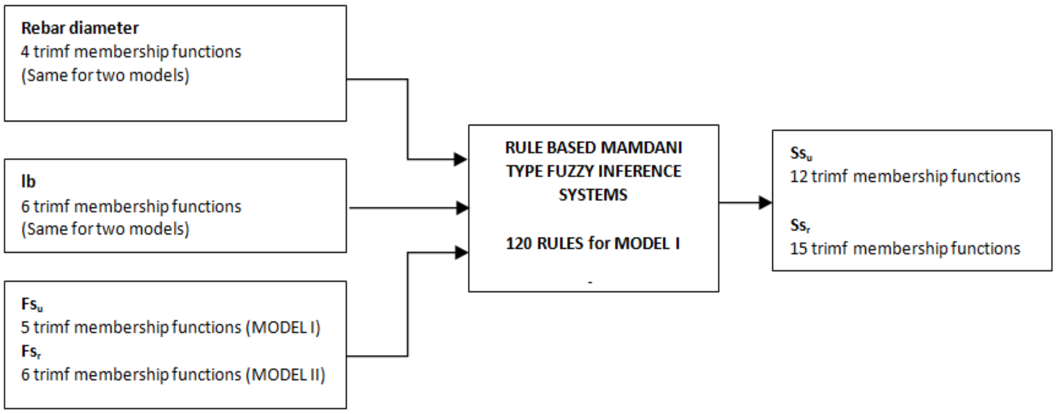

Fig. 5 General structure of the models

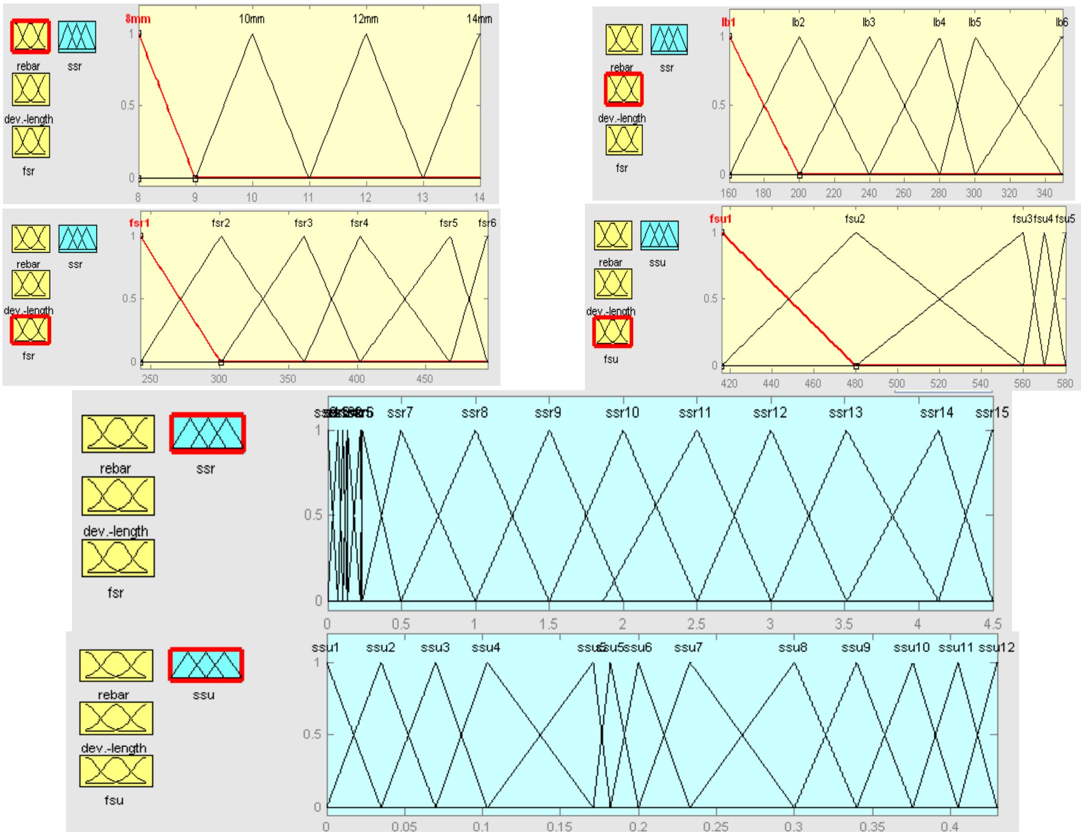

Fig. 6 Inputs and outputs membership functions of the models

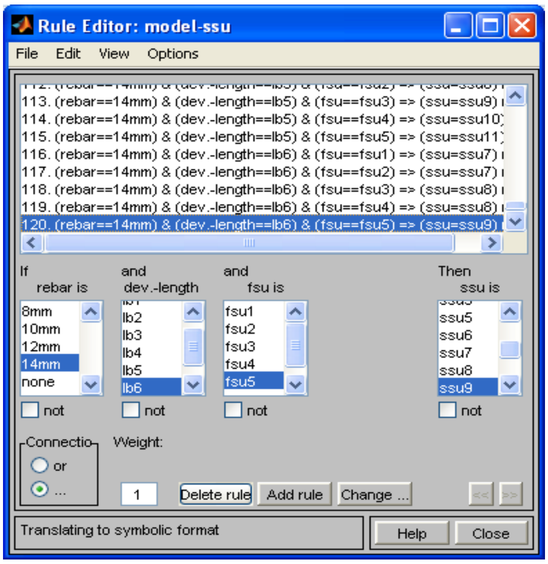

(a) Model I

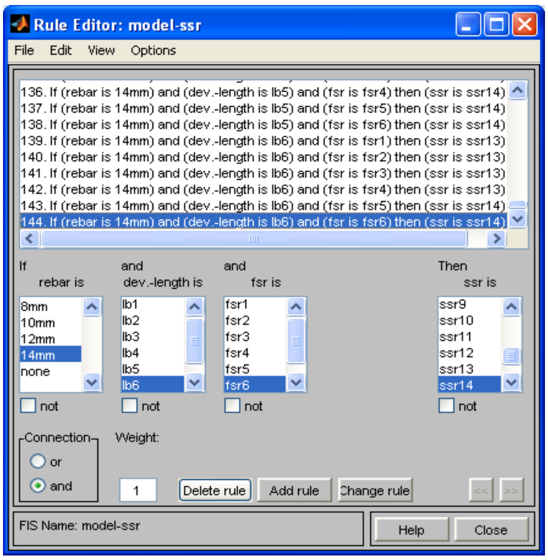

(b) Model II

Fig. 7 Rules editor for two models

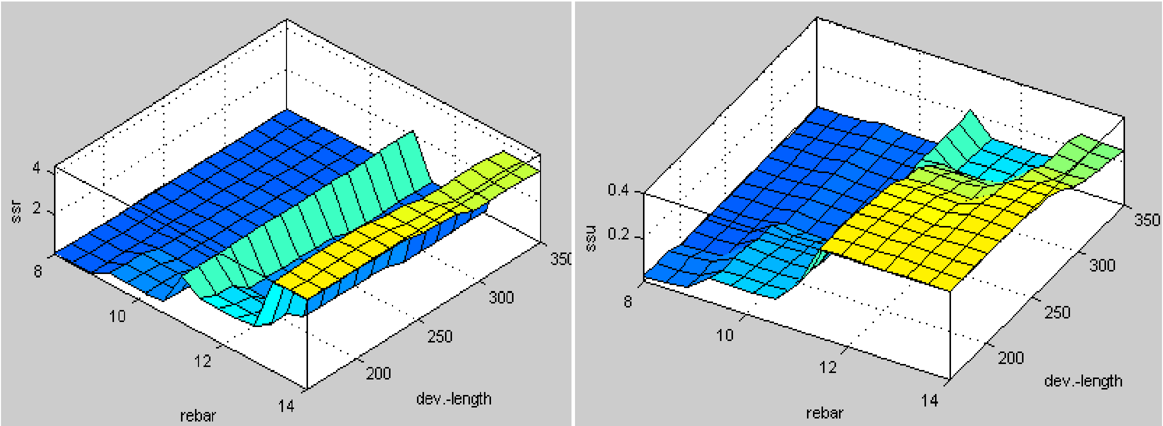

Fig. 8 Output parameters variations as a function of inputs

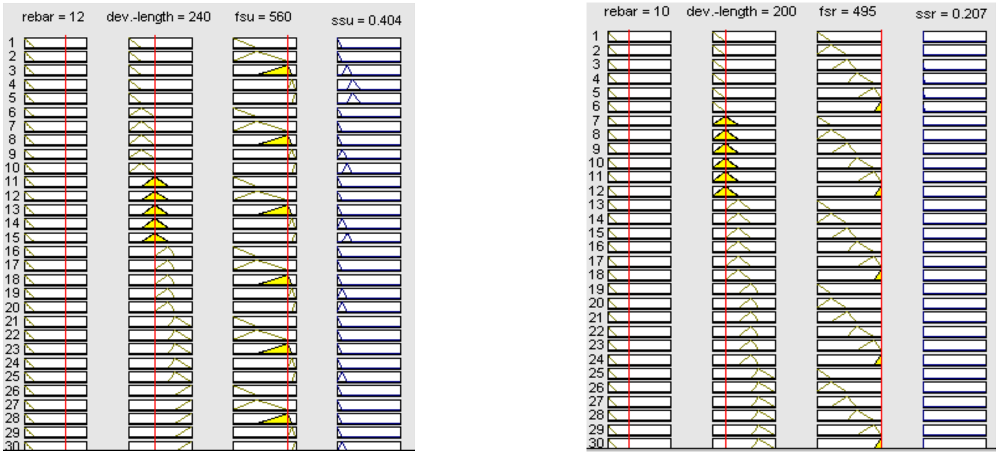

Fig. 9 Defuzzification monitor of the model

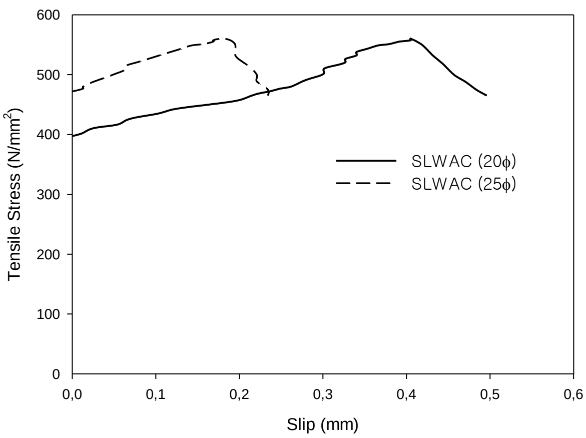

Fig. 10 Typical tensile stress-slip relationships of the experiments (Results of 12 mm diameter rebar)

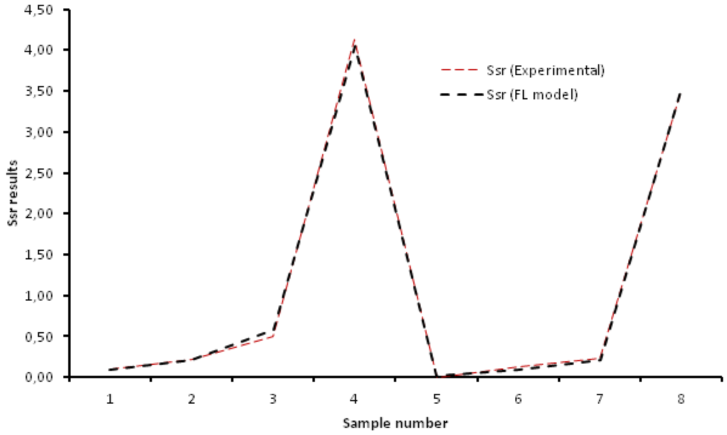

Fig. 11 Matching figure for S_{sr}

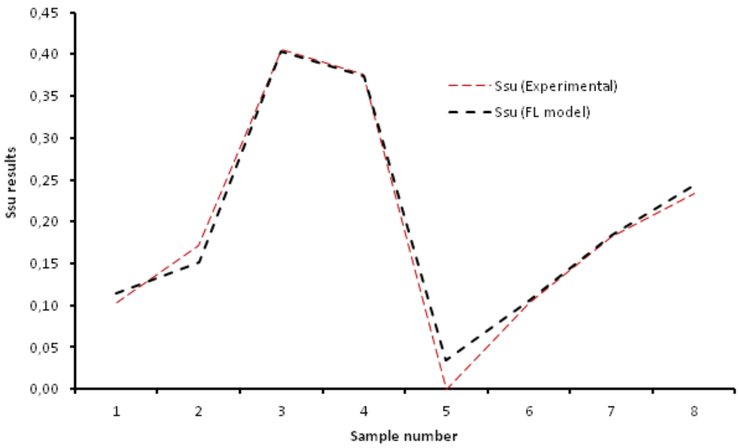

Fig. 12 Matching figure for S_{su}

Table 5 Details of bending tests with both experimental and modeling results

Concrete Type	f_{ck} MPa	Rebar mm	l_b mm	Experimental		Fuzzy logic	
				f_{su}/s_{su} MPa/mm	f_{sr}/s_{sr} MPa/mm	f_{su}/s_{su} MPa/mm	f_{sr}/s_{sr} MPa/mm
SLWC	18.5	8	160	570/0.103	490/0.103	570/0.115	490/0.09
		10	200	580/0.171	495/0.223	580/0.152	495/0.207
		12	240	560/0.405	465/0.496	560/0.404	465/0.577
		14	280	416/0.376	238/4.134	416/0.374	238/4.05
		8	200	570/0	490/0	570/0.0351	490/0.0137
		10	250	580/0.103	495/0.132	580/0.106	495/0.09
		12	300	560/0.182	465/0.234	560/0.184	465/0.207
		14	350	417/0.233	247/3.512	417/0.244	247/3.55

Table 6 Statistical parameters for comparison

SET	Statistical parameters for comparison of the results of developed FL models and experimental	
	R^2	RMSE
MODEL I	0.986009	0.015313
MODEL II	0.999117	0.047653

$$x^* = \frac{\int \mu_i(x)\,x\,dx}{\int \mu_i(x)\,dx} \tag{2}$$

where x^* is the defuzzified output, μ_i(x) is the aggregated membership function and x is the output variable.

As the final stage, after creating the model, the model results were obtained from the defuzzification monitor of the models (Fig. 9). A representative typical tensile stress-slip relationship of the experiments for 12 mm diameter rebar is shown in Fig. 10. Details of bending tests with both experimental and modeling results are given in Table 5.

Here, maximum tensile stress, slippage at maximum tensile stress, tensile stress at rupture and slippage at rupture are shown with f_{su}, s_{su}, f_{sr}, s_{sr}, respectively. Matching figures of experimental and modeling results are given in Fig. 11 and 12 for S_{su} and S_{sr}.

Two statistical evaluation criterias for comparison of the results of the developed FL models and experimental (see in Table 5) were used. These statistical parameters are the coefficient of determination R^2, the Root Mean Square Error (RMSE) defined as follows

$$R^2 = 1 - \left\{ \frac{\sum_{i=1}^{N} \left(Y_{i(m)} - Y_{i(p)} \right)^2}{\sum_{i=1}^{N} \left(Y_{i(m)} - Y_{i(mean)} \right)^2} \right\} \tag{3}$$

$$RMSE = \sqrt{\frac{1}{N} \sum_{i=1}^{N} \left(Y_{i(m)} - Y_{i(p)} \right)^2} \tag{4}$$

Here m represents measured values, p the predicted values, mean is the average of measured values and N is the number of data points. The statistical values of R^2 and RMSE including all the data sets are given in Table 6.

5. Conclusions

The potential of the rule based Mamdani type fuzzy logic model for prediction of slippage at maximum tensile strength (S_{su}) and slippage at rupture (S_{sr}) of structural lightweight concretes according to steel rebar diameters and development length of rebars as inputs has been investigated in this research. Experimental data were used to create the model. After modeling, the results obtained from the developed model compared with the experimental results. The following conclusions can be written for this research:

- Experimental results of beam specimens with SLWC that 20 development length is sufficient for 8 and 10 mm rebars. But this length must be increased for 12 and 14 mm diameter rebars.

- Bond strength of SLWC beam specimens which have 25 development length increased in proportion to 20 development length and provided stress distribution without exceeding their bearing capacity for 8, 10, 12 mm rebars. However, 14 mm rebars still exceeded their bearing capacity by shear forces before yield stress, but maximum amount of slippage was 3.512 mm by decreasing.
- All the tests show that small sized rebars have higher bond strength than bigger ones considerably.
- Results of this investigation show that SBHBT is more convenient for small sized steel rebar (<14 mm for SLWC), because beam specimens don't include stirrups and to reach yield stress higher tensile forces should be applied to rebar. In this way, specimens exceed their bearing capacity by shear forces before yield stress.
- According to the matching figures between model results and experimental results (Fig. 11-12), it can be concluded that the values are close to each other.
- According to the coefficient of determination (R^2) values between model results and experimental results, the values were found 0.986009 for MODEL I, 0.999117 for MODEL II and according to the Root Mean Square Error (RMSE) values, the values were found 0.015313 for MODEL I, 0.047653 for MODEL II. These results show very acceptable relations between developed model results and experimental results.
- As a result, it was shown that the Slippage at maximum tensile strength (s_{su}) and slippage at rupture (s_{sr}) of structural lightweight concretes can be predicted using the rule based FL model in a relatively short period of time.

References

Abraham, A. (2002), *Rule Based Expert Systems, Handbook for Measurement Systems Design, Peter Sydenham and Richard Thorn (Eds.)*, John Wiley and Sons Ltd., London, UK.

ACI 318-05 (2005), *Building Code Requirements for Structural Concrete and Commentary*, USA.

Akkurt, I., Başyiğit, C., Kılınçarslan, S. and Beycioğlu A. (2010), "Prediction of photon attenuation coefficients of heavy concrete by fuzzy logic", *J. Frank. Inst.*, **347**(9), 1589-1597

Arda, T.S. (1968), *Compilation about Bond Behavior in Reinforced Concrete*, I.T.U., Istanbul, Turkey.

Arslan, M.E. (2007), "Investigation of bond strength of structural lightweight concrete and ordinary concrete comparatively in bending", MSc Thesis, Karadeniz Technical University, Trabzon.

Arslan, M.E. and DURMUŞ, A. (2011), "Investigation of bond behavior between lightweight aggregate concrete and steel rebar using bending test", *Comput. Concrete- Int. J.*, **8**(4), 465-472.

Babu, K.G. and Babu, D.S. (1989), Behavior of lightweight expanded polystyrene concrete containing silica fume, *Cement Concrete Res.*, **33**(5), 755-762.

Başyiğit, C., Akkurt, I., Kılınçarslan, S. and Beycioğlu, A. (2010), "Prediction of compressive strength of heavyweight concrete by ANN and FL models", *Neural Comput. Appl.*, **19**(4), 507-513.

Campione, G. and Mendola, L.L. (2004), "Behavior in compression of lightweight fiber reinforced concrete confined with transverse steel reinforcement", *Cement Concrete Compos.*, **26**(6), 645-656.

Chi, J.M., Huang R., Yang, C.C. and Chang, J.J. (2003), "Effect of aggregate properties on the strength and stiffness of lightweight concrete", *Cement Concrete Compos.*, **25**(2), 197-205.

Dahil, H.A. (2001), "Comparative Study of bond strength between steel rebars and high performance and ordinary concrete", MSc Thesis, Karadeniz Technical University, Trabzon.

Ersoy, U. and Özcebe, G. (2001), *Reinforced Concrete: Basic Principles and Designing According to TS-500-2000 and Turkey's Earthquake Resistant Design Code (1998)*, Evrim Publishing, Istanbul, Turkey.

Ferguson, P.M. (1965), *Reinforced Concrete Fundamentals*, Second Edition, John Wiley and Sons, New York, USA.

Hüsem, M. and Durmuş, A. (1993), *Lightweight Aggregate Concretes Produced with Aggregates of Blacksea Region*, Advances in Civil Engineering, First Technical Congress, Book of Proclamation, Gazi Mağusa-KKTC, October.

Hüsem, M. and Durmuş, A. (1995), "Investigation of bond strength of lightweight aggregate concrete and ordinary concrete comparatively", Turkey Civil Engineering XIII. Technical Congress, Istanbul, November.

Hüsem, M. (1995), "Investigation of Lightweight Aggregate Concrete Produced with Aggregate of Blacksea Region and Ordinary Concrete Comparatively", Ph.D. Thesis, Karadeniz Technical University, Trabzon.

Ichinose, T., Kanayama, Y., Inoue, Y. and Bolander, J.E. (2004), "Size effect on bond strength of deformed bars", *Construct. Build. Mater.*, **18**(7), 549-558.

Kayali, O., Haque M.N. and Zhu B. (2003), "Some characteristics of high strength fiber reinforced lightweight aggregate concrete", *Cement Concrete Compos.*, **25**(2), 207-213.

Kılıç, A., Atiş, C.D., Yaşar, E. and Ö zcan F. (2003), "High-strength lightweight concrete made with scoria aggregate containing mineral admixtures", *Cement Concrete Res.*, **33**(10), 1595-1599.

Köksal, F., Şahin, Y., Beycioğlu, A., Gençel, O. and Brostow, W. (2012), "Estimation of fracture energy of high strength steel fiber reinforced concrete using rule based mamdani type fuzzy inference system", *Sci. Eng. Compos. Mater.*, **19**(4), 373-380.

Mounir M.K., Mohamed A.S. and Mohamed A.A. (2013), "Steel-concrete bond potentials in self-compacting Concrete mixes incorporating dolomite powder", *Adv. Concrete Construct., An Int. J.*, **1**(4).

Omid, M. (2011) "Design of an expert system for sorting pistachio nuts through decision tree and fuzzy logic classifier", *Expert Syst. Appl.*, **38**(4), 4339-4347

Subaşı, S., Beycioğlu A., Sancak, E. and Şahin, İ. (2012), "Rule-based mamdani type fuzzy logic model for the prediction of compressive strength of silica fume included concrete using non-destructive test rresults", *Neural Comput. Appl.*, DOI: 10.1007/s00521-012-0879-4.

Topcu, I.B. and Sarıdemir, M. (2008a), "Prediction of compressive strength of concrete containing fly ash using artificial neural network and fuzzy logic", *Comput .Mater. Sci.*, **41**(3), 305-311.

Topcu, I.B. and Sarıdemir, M. (2008b), "Prediction of rubberized concrete properties using artificial neural networks and fuzzy logic", *Construct. Build Mater.*, **22**(4), 532-540.

Yeih, W., Chang, J.J. and Tsai, C.L. (2004), "Enhancement of the bond strength of epoxy coated steel by the addition of fly ash", *Cement Concrete Compos.*, **26**(4), 315-321.

Zadeh, L.A. (1965), "Fuzzy Sets", *Inform. Control*, **8**, 338-352.

CC